

Molecular Insights on the Cyclic Peptide Nanotube-Mediated Transportation of Antitumor Drug 5-Fluorouracil

Huifang Liu,[†] Jian Chen,[†] Qing Shen, Wei Fu,* and Wei Wu*

School of Pharmacy, Fudan University, 826 Zhangheng Road,
Shanghai, 201203, P. R. China

Received August 19, 2010; Revised Manuscript Received October 11, 2010; Accepted
October 21, 2010

Abstract: Self-assembled cyclic peptide nanotubes (CPNs) show a potential use in drug delivery. In this study, the CPN composed of (Trp-D-Leu)₄-Gln-D-Leu was synthesized and tested for the transport of the antitumor drug 5-fluorouracil (5-FU). CPN-mediated release of 5-FU from liposomes experimentally tested the transportation function of the synthetic CPNs. To explore the transportation mechanism of CPNs, computational studies have been performed on the CPN models stacked by 8 subunits, including conventional molecular dynamics (CMD) simulations, and steered molecular dynamics (SMD) simulations in the environment of hydrated dimyristoylphosphatidylcholine (DMPC) lipid bilayer. Our CMD simulations demonstrated that the *ortho*-CPN is the most stable nanotube, in which the Gln residue is in the *ortho*-position relative to other residues. The calculated diffusion coefficient value for inner water molecules was $1.068 \times 10^{-5} \text{ cm}^2 \cdot \text{s}^{-1}$, almost half that of the bulky water and 24 times faster than that of the typical gramicidin A channel. The CPN conserved its hollow structure along the 10 ns CMD simulations, with a tilt angle of 50° relative to the normal of DMPC membrane. Results from SMD simulations showed that the 5-FU molecule was transported by hopping through different potential energy minima distributed along subunits, and finally exited the nanotube by escaping from the kink region at the last two subunits. The hopping of 5-FU was driven by switching from hydrophobic interactions between 5-FU and the interior wall of the nanotube to hydrogen bonding interactions of 5-FU with the backbone carbonyl group and amide group of *ortho*-CPN. The calculated binding free energy profile of 5-FU interacting with the CPN indicated that there was an energy well near the outer end of the nanotube.

Keywords: 5-fluorouracil; Cyclic peptide nanotube; steered molecular dynamics; drug transporter; antitumor

Introduction

Malignant tumor is the most severe disease threatening the health of human beings. More and more antitumor drugs have been discovered. However, the biggest problem is that these drugs could not efficiently exhibit their activity in killing tumors due to the difficulty in their ability to penetrate through the cell membrane.¹ Synthetic cyclic peptide nano-

tubes are emerging as promising and selective drug transporters. Our preliminary *in vitro* and *in vivo* studies have demonstrated that the synthetic decapeptide tube could efficiently enhance the antitumor potency of 5-fluorouracil (5-FU) (unpublished data).

Cyclic peptide nanotubes (CPNs) are a class of artificial channels formed by closed peptide rings which consist of an even number of alternating D- and L-amino acid residues.²

* Corresponding authors. E-mail: wfu@fudan.edu.cn (W.F.), wuwe@fudan.edu.cn (W.W.). Mailing address: Fudan University, School of Pharmacy, 826 Zhangheng Road, Shanghai, 201203, P. R. China. Fax: +86-21-51980010. Phone: +86-21-51980010.

[†] These authors contributed equally to this work.

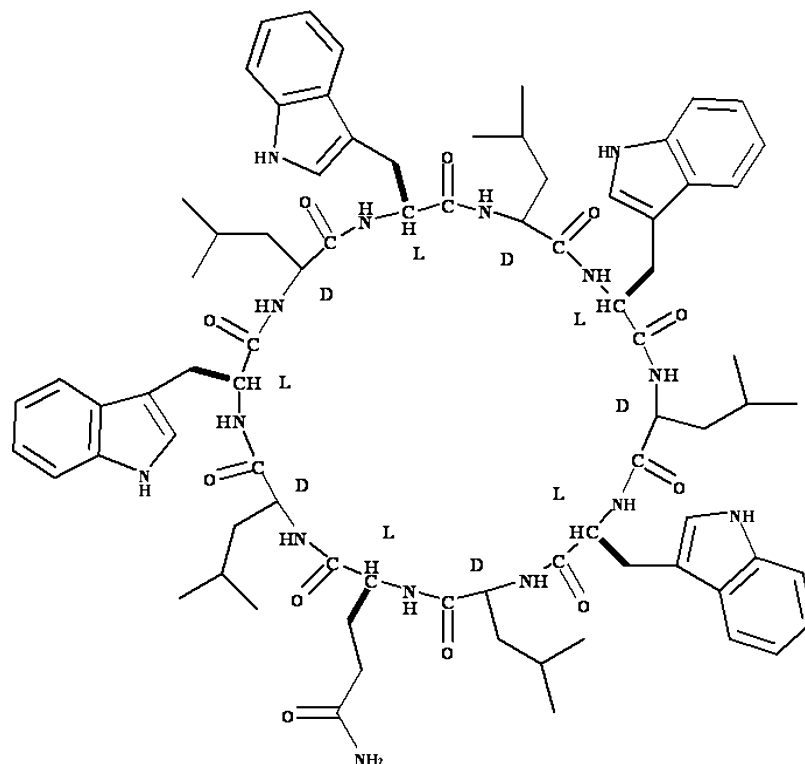
(1) Adson, A.; Burton, P. S.; Raub, T. J.; Barsuhn, C. L.; Audus, K. L.; Ho, N. F. Passive diffusion of weak organic electrolytes across Caco-2 cell monolayers: uncoupling the contributions of hydrodynamic, transcellular, and paracellular barriers. *J. Pharm. Sci.* **1995**, *84* (10), 1197–1204.

By simply adjusting the number and kinds of amino acid residues, both the internal diameter and external surface properties can be tailored. Generally, the interior surface of such a tube is hydrophilic as indicated by the presence of water molecules, while the exterior surface is hydrophobic, permitting facile dissolution in nonpolar solvents.³ A network of hydrogen bonds between oxygen atoms of the participating carbonyl groups and amino groups at the backbone of adjacent cyclic peptide subunits drives them into a quasi- β -strand self-assembled tubular structure.⁴ The internal diameter of the nanotube could be adjusted by simply varying the size of the peptide ring. Electron diffraction analysis indicated that the tightly hydrogen-bonded rings stacked with an average intersubunit distance of ~ 4.7 Å.⁵ The cyclic D,L-peptides with appropriate hydrophobic side chains can self-assemble and insert into lipid bilayers, and finally transport ions or guest molecules across the membrane.⁶

Studies on CPNs began from the year of 1974 and became a hot research topic in the area of ion or small molecule transportation.⁷ Both experimental and theoretical studies on CPNs have been devoted to an understanding of their structural and dynamical characteristics, and transportation properties.^{8–10} In 1993, Ghadiri et al. reported the first well-characterized structure of self-assembled cyclic octapeptide subunits *cyclo*[-(D-Ala-Glu-D-Ala-Gln)₂-] in crystalline nanotubular arrays, convincingly establishing that the ring-shaped subunits can stack through antiparallel β -sheet hydrogen bonds to form hollow tubes.¹¹ Later, Lambert and co-workers demonstrated their result by the IR spectrum and morphology of the crystals formed by *cyclo*[-(Asn-D-Phe-

Asp-D-Phe)₂-].¹² In 1998, studies by polarized attenuated total reflectance infrared (ATR-IR) spectroscopy showed that CPNs oriented themselves in a transport-competent membrane orientation.¹³ The cyclic peptide nanotubes could act as highly selective and efficient transmembrane channels for ions and small molecules.¹⁴ In 1994, Ghadiri confirmed that the synthetic decapeptide *cyclo*[-(Trp-D-Leu)₄-Gln-D-Leu-] has the function of glucose transportation.¹⁵ Since then, atomic-level theoretical and computational work has helped to better understand the characteristics of structure, dynamics and transport activity of the cyclic peptide nanotubes. Engels et al. found that cyclic D,L-octapeptide could self-assemble as nanotubes. The diffusion of water molecules inside that peptide nanotube was much faster than that inside the gramicidin A channel.¹⁶ Asthagiri et al. calculated the solvation free energies of Li⁺, Na⁺, Rb⁺ and Cl⁻ inside a self-assembled (D,L)-octapeptide nanotubes using MD-based perturbation free energy calculations;¹⁷ Tarek et al. found that peptide nanotubes could tilt along the normal of lipid bilayer after the nanotubes were equilibrated, but the hollow tubular structure was conserved;¹⁸ Hwang et al. calculated the free energy barrier for Na⁺ and K⁺ ions diffusing through the cyclic peptide nanotube to be ~ 2.4 kcal/mol, and found that the carbonyl groups of the cyclic peptide were structurally rigid because of the network of hydrogen bonding.¹⁹ All these studies confirmed that cyclic peptide readily self-assembles to be a nanotube with a potential transportation function. The questions are how the size and kind of peptide determine the properties of a nanotube, and how the assembled nanotube transports guest molecules like drugs. Answers to these questions have great significance and potential applications in the area of drug delivery.

- (2) Ghadiri, M. R. Self-assembled nanoscale tubular ensembles. *Adv. Mater.* **1995**, *7* (7), 675–677.
- (3) Buriak, J. M.; Ghadiri, M. R. Self-assembly of peptide based nanotubes. *Mater. Sci. Eng.: C* **1997**, *4* (4), 207–212.
- (4) Karlstrom, A.; Unden, A. Association of cyclic peptides in aqueous solution measured by fluorescence quenching. *Biopolymers* **1997**, *41* (1), 1–4.
- (5) Hartgerink, J. D.; Granja, J. R.; Milligan, R. A.; Ghadiri, M. R. Self-assembling peptide nanotubes. *J. Am. Chem. Soc.* **1996**, *118* (1), 43–50.
- (6) Ghadiri, M. R.; Granja, J. R.; Buehler, L. K. Artificial Transmembrane Ion Channels from Self-Assembling Peptide Nanotubes. *Nature* **1994**, *369* (6478), 301–304.
- (7) Desantis, P.; Morosett, S.; Rizzo, R. Conformational-Analysis of Regular Enantiomeric Sequences. *Macromolecules* **1974**, *7* (1), 52–58.
- (8) Liu, Z. W.; Xu, Y.; Tang, P. Steered molecular dynamics simulations of Na⁺ permeation across the gramicidin a channel. *J. Phys. Chem. B* **2006**, *110* (25), 12789–12795.
- (9) Chen, G. J.; Su, S. J.; Liu, R. Z. Theoretical studies of monomer and dimer of *cyclo*[-L-Phe¹-D-Ala²-]_n and *cyclo*[-L-Phe¹-D-Meⁿ-N-Ala²-]_n ($n = 3-6$). *J. Phys. Chem. B* **2002**, *106* (7), 1570–1575.
- (10) Lewis, J. P.; Pawley, N. H.; Sankey, O. F. Theoretical investigation of the cyclic peptide system *cyclo*[(D-Ala-Glu-D-Ala-Gln)_{m=1-4}]. *J. Phys. Chem. B* **1997**, *101* (49), 10576–10583.
- (11) Ghadiri, M. R.; Granja, J. R.; Milligan, R. A.; McRee, D. E.; Khazanovich, N. Self-Assembling Organic Nanotubes Based on a Cyclic Peptide Architecture. *Nature* **1993**, *366* (6453), 324–327.
- (12) Polaskova, M. E.; Ede, N. J.; Lambert, J. N. Synthesis of nanotubule-forming cyclic octapeptides via an Fmoc strategy. *Aust. J. Chem.* **1998**, *51* (7), 535–540.
- (13) Kim, H. S.; Hartgerink, J. D.; Ghadiri, M. R. Oriented self-assembly of cyclic peptide nanotubes in lipid membranes. *J. Am. Chem. Soc.* **1998**, *120* (18), 4417–4424.
- (14) Sanchez-Quesada, J.; Ghadiri, M. R.; Bayley, H.; Braha, O. Cyclic peptides as molecular adapters for a pore-forming protein. *J. Am. Chem. Soc.* **2000**, *122* (48), 11757–11766.
- (15) Ashkenasy, G.; Ghadiri, M. R. Boolean logic functions of a synthetic peptide network. *J. Am. Chem. Soc.* **2004**, *126* (36), 11140–11141.
- (16) Granja, J. R.; Ghadiri, M. R. Channel-Mediated Transport of Glucose across Lipid Bilayers. *J. Am. Chem. Soc.* **1994**, *116* (23), 10785–10786.
- (17) Engels, M.; Bashford, D.; Ghadiri, M. R. Structure and Dynamics of Self-Assembling Peptide Nanotubes and the Channel-Mediated Water Organization and Self-Diffusion—A Molecular-Dynamics Study. *J. Am. Chem. Soc.* **1995**, *117* (36), 9151–9158.
- (18) Asthagiri, D.; Pratt, L. R.; Ashbaugh, H. S. Absolute hydration free energies of ions, ion-water clusters, and quasichemical theory. *J. Chem. Phys.* **2003**, *119* (5), 2702–2708.
- (19) Tarek, M.; Mairret, B.; Chipot, C. Molecular dynamics investigation of an oriented cyclic peptide nanotube in DMPC bilayers. *Biophys. J.* **2003**, *85* (4), 2287–2298.
- (20) Hwang, H.; Schatz, G. C.; Ratner, M. A. Steered molecular dynamics studies of the potential of mean force of a Na⁺ or K⁺ ion in a cyclic peptide nanotube. *J. Phys. Chem. B* **2006**, *110* (51), 26448–26460.

Scheme 1. Two-Dimensional Structure of the $cyclo[-(Trp-D-Leu)_4-Gln-D-Leu-]$ Peptide

In this work, we synthesized the $cyclo[-(Trp-D-Leu)_4-Gln-D-Leu-]$ subunit, performed dialysis studies of 5-FU-loaded liposomes in the environment of cyclic peptide solution, and investigated the antitumor activity by means of *in vitro* studies. Based on our preliminary experimental findings we examined the structural and dynamical characteristics of CPNs in a fully hydrated dimyristoylphosphatidylcholine (DMPC) lipid bilayer by conventional molecular dynamics (CMD) simulations. The transportation mechanism of 5-FU by the CPNs is explored by means of steered molecular dynamics (SMD) simulations. Our results show that synthetic CPN is able to efficiently transport the drug 5-FU by hopping the 5-FU molecule through different energy minima along the nanotube. Our findings are helpful for the design of more efficient drug delivery vehicles.

Experimental Methods

Synthesis of $cyclo[-(Trp-D-Leu)_4-Gln-D-Leu-]$ Peptide and Transportation Test. $cyclo[-(Trp-D-Leu)_4-Gln-D-Leu-]$ peptide (as shown in Scheme 1) was synthesized and cyclized by a traditional solid-phase synthesis strategy.²⁰ Briefly, the linear decapeptide was assembled by standard Boc chemistry in the solid phase and subsequently cyclized in solution with high efficiency and reproducibility. L-Glutamine was adopted in the amino acid sequence for the convenience of the peptide synthesis. The synthetic cyclic

peptide was analyzed by reverse phase high performance liquid chromatography (RP-HPLC) in order to determine the end point of the cyclization reaction, and the crude product was purified by semipreparative RP-HPLC. Finally, the cyclized peptide was structurally analyzed by ESI-MS and ¹H NMR. CPN-mediated transportation of 5-FU from liposomes was studied by an *in vitro* dialysis method. First, 5-FU-loaded liposomes and cyclic peptides in dilute DMF solution were sealed in a dialysis bag and dialyzed against phosphate buffer saline (pH 7.3) as the receptor phase (30 mL, 37 °C, 100 rpm) within a period of 90 min. The release of 5-FU was tested at 2 mg/mL concentrations of the cyclic peptides. The amount of the released 5-FU was quantified at each time interval by HPLC. The mean values of six replicates were reported.

Description of the Model Systems. The structural model of $cyclo[-(Trp-D-Leu)_4-Gln-D-Leu-]$ nanotube was built according to Ghadiri's model and modified according to the X-ray crystallographic structures of related peptide ensembles^{11,18,21} by using Sybyl 6.9 software (Tripos Inc., St. Louis, MO). Although our experiments did not determine the exact number of subunits in one CPN nanotube, we selected the CPN assembly of 8 peptide subunits in order to roughly match the thickness of the DMPC bilayer. All the side chains of the 8 peptides point outward attributed to their alternated D and L chirality. As the L-Gln could have three

(20) Chen, J.; Zhang, B.; Xie, C.; Lu, Y.; Wu, W. Synthesis of a highly hydrophobic cyclic decapeptide by solid-phase synthesis of linear peptide and cyclization in solution. *Chin. Chem. Lett.* **2010**, *21* (4), 391–394.

(21) Zhu, J. C.; Cheng, J.; Liao, Z. X.; Lai, Z. H.; Liu, B. Investigation of structures and properties of cyclic peptide nanotubes by experiment and molecular dynamics. *J. Comput.-Aided Mol. Des.* **2008**, *22* (11), 773–781.

different positions relative to other amino acids in the peptide chain, namely the *ortho*-position, *meta*-position and *para*-position, the 8 cyclic peptides are stacked in three possible low-energy modes (see Figure S1 in the Supporting Information). Therefore, three low-energy stacking models of CPN were constructed. For each CPN, the interior tube diameter is 10 Å, the side chains of L-Trp and the D-Leu are distributed uniformly, and the center-to-center distance between neighboring subunits is 4.75 Å. For convenience, the nanotube subunits are numerically denoted. As displayed in Figure S1 in the Supporting Information, APR (α -plane region) represents the plane of C α atoms along one peptide subunit, while MPR (midplane region) represents the region between two APRs. The whole length of one CPN is 38.7 Å according to the distance from APR1 to APR8.

Conventional Molecular Dynamics Simulation. After each of the three CPNs (i.e., *ortho*-CPN, *meta*-CPN and *para*-CPN) was built, it was inserted into the fully hydrated DMPC bilayer by aligning the axis of CPN to the normal of the lipid bilayer. The process of aligning CPN with the normal of the DMPC membrane was similar to those used in our previous membrane protein simulations.²² When solvating the CPN/DMPC system, 42 Na⁺ and 42 Cl⁻ ions were added in order to simulate the 150 mM physiological ion strength. The size of the whole solvated system was 77 Å \times 83 Å \times 110 Å, including one CPN, 189 DMPC molecules and 15087 water molecules.

Energy minimizations were performed for each of the three CPN/DMPC/water systems, first for all water molecules, then for the whole system until the maximum force became smaller than 10.00 kcal/mol \cdot Å. The energy-minimized CPN/DMPC/water system was then subjected to MD simulation. The MD simulations were performed by using the GROMACS package version 3.3.3 with the GROMOS96 force field.²³

The solvent (water and DMPC) molecules of each initial system were equilibrated with CPN structures by constraining the solute (CPNs) at 300 K for 20 ps. Then the CPN was equilibrated for 5 ps while the solvent molecules were constrained at 10, 50, 100, 200, and 298 K. Afterward, each system was equilibrated for 500 ps without any constraints. To maintain the systems at a constant temperature of 300 K, the Berendsen thermostat²⁴ was applied using a coupling time of 0.1 ps for the bulk water and DMPC. The pressure was maintained by coupling to a reference pressure of 1 bar. The values of the anisotropic isothermal compressibility were

set to 4.5×10^{-5} , 4.5×10^{-5} , 4.5×10^{-5} , 0, 0, 0 bar⁻¹ for *xx*, *yy*, *zz*, *xy/yx*, *xz/zx* and *yz/zy* components for water and DMPC simulations. All bond lengths, including those to hydrogen atoms, were constrained by the LINCS algorithm.²⁵ Electrostatic interactions between charged groups within 9 Å were calculated explicitly, while long-range electrostatic interactions were calculated using the Particle-Mesh Ewald method²⁶ with a grid width of 1.2 Å and a fourth-order spline interpolation. A cutoff distance of 14 Å was applied for the Lennard-Jones interactions. Numerical integration of the equations of motion used a time step of 2 fs with atomic coordinates saved every 1 ps for later analysis. Finally, three 10 ns MD simulations were performed on these systems under the periodic boundary conditions in the NPT canonical ensemble.

Constant Velocity SMD Simulations. The SMD has proved as an effective computational approach to simulate the transportation process of a small molecule permeating through a protein channel.⁸ In SMD simulations, a guest molecule or an ion of interest is steered by an imaginary atomic force microscopy (AFM) tip, and the time-dependent external force is added on the guest molecule to facilitate its transportation through the channel. In the present study, we performed SMD simulations in order to explore how the 5-FU molecule is transported by the CPN channel. In detail, 5-FU was pulled through the tube of the CPN by employing an artificial harmonic force on the center of mass (COM) of 5-FU along the longitudinal axis of the CPN (Figure 1). 5-FU molecule was first placed on the top of CPN, 1.27 nm from the center of subunit 1, and then the whole system was equilibrated for 1 ns. The molecular topology file for 5-FU was generated by the PRODRG server (<http://davapc1.bioch.dundee.ac.uk/prodrg/>).²⁷ The partial atomic charges of 5-FU were determined with the DFT/B3LYP/6-311G** basis set by using the CHelpG method implemented in GAMESS program.²⁸ To avoid large fluctuation in the position, a stiff spring (280 pN \cdot Å) rather than a soft spring was assigned to 5-FU.¹⁹ It should be pointed out that the pulling velocity (V_{pull}) is an important parameter in our SMD simulations. Higher pulling velocity may lead to remarkable nonequilibrium effects, resulting in obvious errors of the simulation results. Very low velocity will make the SMD simulations extremely time-consuming, thus computationally not doable. To find an appropriate pulling velocity, five SMD simulations were performed using different pulling velocities (0.1 Å \cdot ps⁻¹, 5 \times

(22) Fu, W.; Shen, J. H.; Luo, X. M.; Zhu, W. L.; Cheng, J. G.; Yu, K. Q.; Briggs, J. M.; Jin, G. Z.; Chen, K. X.; Jiang, H. L. Dopamine D1 receptor agonist and D2 receptor antagonist effects of the natural product (-)-stapholidine: Molecular Modeling and dynamics Simulations. *Biophys. J.* **2007**, *93* (5), 1431–1441.

(23) Vandrunen, R.; Vanderspoel, D.; Berendsen, H. J. C. GROMACS—a software package and parallel computer for molecular dynamics. In *Abstracts of Papers*, 209th National Meeting of the American Chemical Society; American Chemical Society: Washington, DC; 1995; p 49-COMP. Daura, X.; Mark, A. E.; van Gunsteren, W. F. Parametrization of aliphatic CH_n united atoms of GROMOS96 force field. *J. Comput. Chem.* **1998**, *19* (5), 535–547.

(24) Berendsen, H. J. C.; Postma, J. P. M.; Vangunsteren, W. F.; Dinola, A.; Haak, J. R. Molecular dynamics with coupling to an external bath. *J. Chem. Phys.* **1984**, *81* (8), 3684–3690.

(25) Hess, B.; Bekker, H.; Berendsen, H. J. C.; Fraaije, J. LINCS: A linear constraint solver for molecular simulations. *J. Comput. Chem.* **1997**, *18* (12), 1463–1472.

(26) Darden, T.; York, D.; Pedersen, L. Particle Mesh Ewald—an N.Log(N) Method for Ewald Sums in Large Systems. *J. Chem. Phys.* **1993**, *98* (12), 10089–10092.

(27) Schuettelkopf, A. W.; van Aalten, D. M. F. PRODRG—a tool for high-throughput crystallography of protein-ligand complexes. *Acta Crystallogr.* **2004**, *D60*, 1355–1363.

(28) Bode, B. M.; Gordon, M. S. MacMolPlt: A graphical user interface for GAMESS. *J. Mol. Graphics Modell.* **1998**, *16* (3), 133.

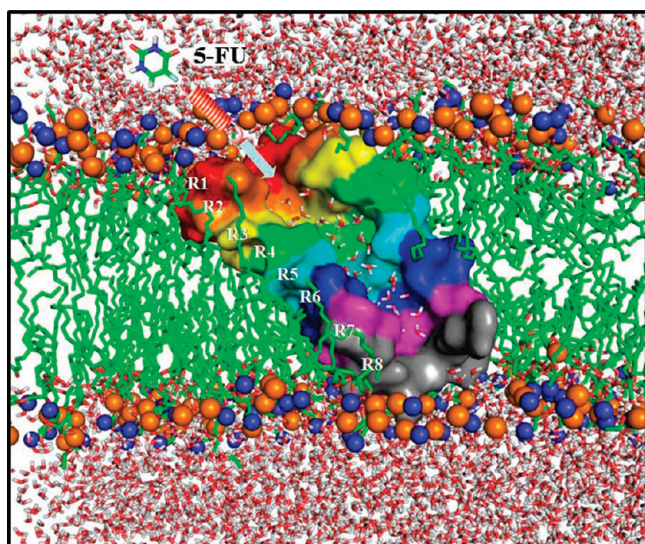


Figure 1. Representative of initial CPN/DMPC/water system for SMD simulation. The front half of the bilayer and subunits are sliced away to display a view of the inner wall of the tube, and the tube molecular surface of each subunit is shown in a different color. 5-FU is shown as stick, which was pulled into the tube along the tube axis through a harmonic potential (spring and arrow). The nitrogen and oxygen of the choline and phosphate are shown as blue and orange balls; the other atoms of the lipid as well as water molecules are represented as sticks.

$10^{-2} \text{ \AA} \cdot \text{ps}^{-1}$, $1 \times 10^{-2} \text{ \AA} \cdot \text{ps}^{-1}$, $5 \times 10^{-3} \text{ \AA} \cdot \text{ps}^{-1}$, $2.5 \times 10^{-3} \text{ \AA} \cdot \text{ps}^{-1}$). Our testing results showed that a SMD simulation with the pulling velocity in the range of $2.5 \times 10^{-3} \text{ \AA} \cdot \text{ps}$ to $0.1 \text{ \AA} \cdot \text{ps}^{-1}$ produced a similar force profile. Herein, the trajectories at minimum velocity $2.5 \times 10^{-3} \text{ \AA} \cdot \text{ps}^{-1}$ was adopted to illustrate the CPN-mediated transportation mechanism of 5-FU.

Results and Discussion

Experimentally Observed 5-FU Transportation by CPN Nanotube. *cyclo*[-(Trp-D-Leu)₄-Gln-D-Leu-] subunits were synthesized by a two-step solid-phase/solution synthesis strategy with a purity of over 98% and were structurally characterized by ¹H NMR and mass spectrometry.²⁰ The absorption, fluorescence spectrophotometry and gel permeation studies⁶ have shown that the synthetic cyclic peptides tend to self-assemble and diffuse into lipid bilayers due to the hydrophobic interactions of their side chains with the hydrophobic chains of lipid when it is distributed into aqueous suspension of liposomes. Our dialysis experiments test such an assembling and insertion process. The release percentage of 5-FU from drug-loaded liposomes after adding cyclic peptides is shown in Figure 2. It can be seen that only 5% of 5-FU diffused from liposomes without cyclic peptides. In contrast, nearly 70% of 5-FU was released into the solution when the concentration of cyclic peptide increased to 2 mg/mL. A similar profile was found for the diffusion of glucose across the CPNs.¹⁵ Similarly, the first-order transport rate constant *k* and average transport rate *v* in 90 min were much higher than that of the control group (without cyclic peptides)

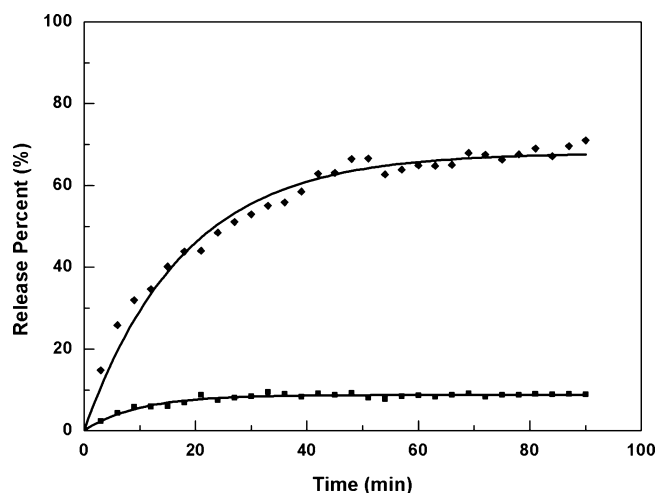


Figure 2. Transportation profiles of 5-FU mediated by cyclic peptides. The transportation of 5-FU is represented in terms of the accumulated transport percentage of drugs as a function of time. The concentration of the cyclic peptides was $35 \mu\text{M}$ (◆); the molar ratio of cyclic peptides to total phosphatidylcholine and cholesterol was 1:600. The control group (■) was without cyclic peptides. The results were presented as raw data.

Table 1. The First-Order Rate Constant *k* (min^{-1}) and Average Transport Rate *v* (nmol/min) of 5-FU in 90 min

concn of CP (μM)	<i>k</i> (min^{-1})	<i>v</i> (nmol/min)
0	0.0004	12.09 ± 2.06
35 ^a	0.0114	140.56 ± 19.45

^a The concentration of cyclic peptide in its solvent DMF, whose final molar ratio to total phosphatidylcholine and cholesterol in the released system is 1:600.

(Table 1). The presence of a small amount of DMF has no significant effect on 5-FU transportation rate. The observed linear relation between transport rate and 5-FU concentration strongly supports a simple transmembrane channel-mediated transportation process. Moreover, studies on three kinds of carcinoma cell lines *in vitro* and the mice inoculated with S180 solid tumor *in vivo* demonstrated that the administration of cyclic peptide nanotubes efficiently enhanced the antitumor activity of 5-FU (unpublished data). All of these experiments demonstrate that the synthetic cyclic peptides stack and self-assemble into tubes, followed by their insertion into the liposome membrane and transportation of antitumor drug 5-FU across the liposome membrane.

The *ortho*-CPN Is the Most Stable Self-Assembled Nanotube. The conventional CMD simulations for 3 model systems were conducted to investigate the structural and dynamical properties of synthesized CPN. The 10 ns CMD simulations showed that *ortho*-CPN, *meta*-CPN and *para*-CPN behaved differently in explicitly hydrolyzed DMPC bilayer. As shown in Figure S2 in the Supporting Information, *meta*-CPN sustained the hollow structure at the beginning, but it began to bend at ~ 2.6 ns and kept the curving posture in the rest of simulation. For *para*-CPN, the tube started to collapse during the first 1 ns simulation and completely collapsed at the end, demonstrating *para*-CPN

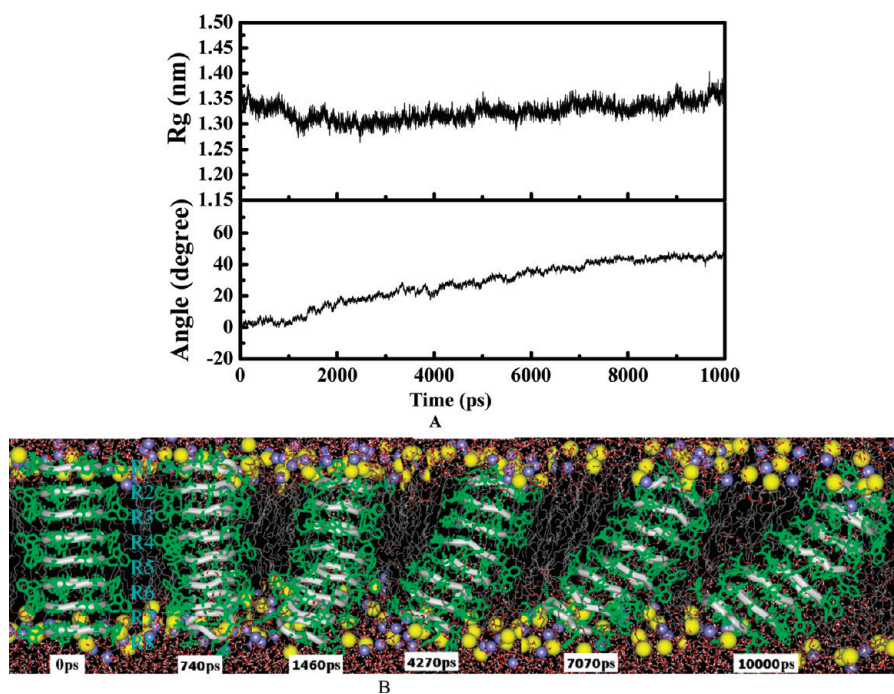


Figure 3. (A) The time-evolutionary radius of gyration (R_g , a measure of the compactness of the protein) and tilt-angle with respect to the normal of bilayer for the self-assembled *ortho*-CPN. (B) Conformational transition of the *ortho*-CPN within the course of the simulation.

was quite unstable. When checking the structures from CMD simulations, we found that the internal hydrogen bonding network (see Figure S3 in the Supporting Information) of *para*-CPN collapsed finally. The *ortho*-CPN retains a hollow tubular structure with only slight distortion at the outer end and has tilted ca. 50° compared with its starting orientation. Such an extent of tilt is close to the reported tilt angle of 39° for *cyclo*[(L-Trp-D-Leu)₃-L-Gln-D-Leu] by ATR-IR spectroscopy measurements.¹⁸ Slight structural distortion was also reported at the outer end of the octapeptide tube.¹⁸ Based on our CMD simulations, the *ortho*-CPN was selected as the starting structure for our SMD simulations, and further structural analysis was performed only for this nanotube.

Along the course of CMD simulation, the average inter-subunit distance for *ortho*-CPN was within the range of 4.73 Å to 4.79 Å. Such an average distance is in good agreement with the reported distance (4.73 Å) from Fourier-transform infrared spectroscopy, electron diffraction and X-ray crystallographic analyses on *cyclo*[-(Gln-D-Ala-Glu-D-Ala)₄] CPN.⁵ The backbone R_g profile (Figure 3A) also supports the structural stability of *ortho*-CPN. A further look at the snapshots of CMD on *ortho*-CPN (Figure 3B) showed that it began to tilt at 1 ns, causing a slight kink in R7 at 1.4 ns. The tilt angle reached 45° at ~ 4.2 ns. The extent of such a tilt kept within the range of $45\text{--}50^\circ$ at the rest of the CMD simulations (Figure 3). As observed, the subunits R7 and R8 tilted more than the other subunits 1 to 6.

Previous study demonstrated that the backbone hydrogen bond network formed by C=O and N-H groups between different subunits are essential for the structural stability of the tube.²⁹ Such a hydrogen bond network in our *ortho*-CPN was relatively persistent during the course of CMD simula-

tion. Interestingly, the side chains of the eight intersubunit peptides rearranged their orientations and have led to the formation of a new hydrogen bond network in consecutive rings, particularly between L-Trp and L-Gln or between L-Gln and L-Gln. This suggests that Gln residue helps to stabilize the tubular arrays, which is in accord with the findings in a previously reported study.³⁰

Water Molecules inside the *ortho*-CPN Nanotube.

During the CMD simulations, water molecules increasingly diffused into the hollow cylindrical tube and flowed smoothly through the whole tube. The average number of water molecules inside the *ortho*-CPN was 38 ± 5 . As shown in Figure 4, there are about 4–5 water molecules in each MPR layer and 1–2 water molecules at each APR. As reported,^{16,18} octapeptide nanotube could hold only ~ 20 water molecules with a typical “1–2” water structure (i.e., APR-1; MPR-2) inside the tube. Such a difference in the number of water molecules mainly comes from the different size of the nanotube. The diameter of our *ortho*-CPN is 10 Å, much larger than that of the octapeptide tube. The MPR water number is bigger than that of APR, because the water molecules at MPR formed hydrogen bonds with the hydrophilic C=O and N-H backbone of the tube wall. The calculated diffusion coefficient value for water molecules inside the *ortho*-CPN is $1.068 \times 10^{-5} \text{ cm}^2 \cdot \text{s}^{-1}$, almost half of the diffusion coefficient value of bulky

(29) Jingchuan, Z.; Jie, C.; Zhouxiang, L.; Zhonghong, L.; Bo, L. Investigation of structures and properties of cyclic peptide nanotubes by experiment and molecular dynamics. *J. Comput.-Aided Mol. Des.* **2008**, *22*, 773–781.

(30) Jillian, M.; Buriak, M.; Reza, G. Self-assembly of peptide based nanotubes. *Mater. Sci. Eng.: C* **1997**, *4*, 207–212.

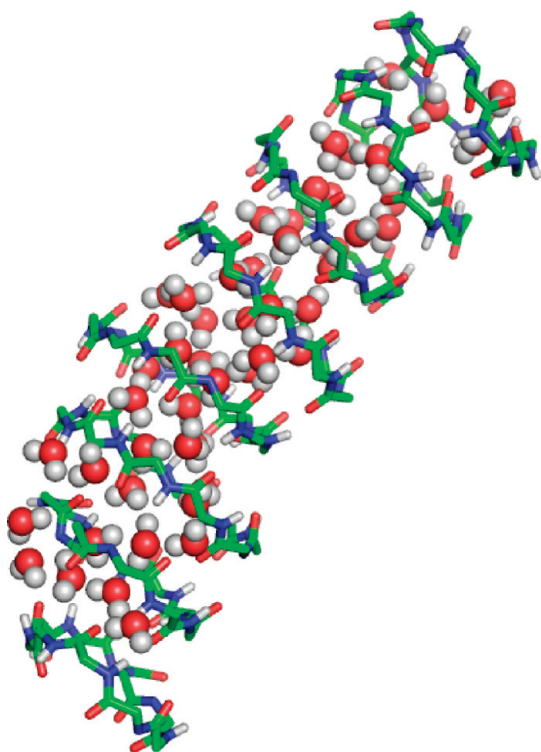


Figure 4. The structure of the internal diffusing water molecules in the *ortho*-CPN nanotubes.

water molecules (calculated as $2.181 \times 10^{-5} \text{ cm}^2 \cdot \text{s}^{-1}$ and experimentally determined as $2.3 \times 10^{-5} \text{ cm}^2 \cdot \text{s}^{-1}$ at $T = 298 \text{ K}$).³¹ As a water channel, the calculated water diffusion coefficient value was reported as $1.068 \times 10^{-5} \text{ cm}^2 \cdot \text{s}^{-1}$, and the calculated water diffusion coefficient value for *cyclo*[(Trp-D-Leu)₃-Gln-D-Leu] channel was only $0.44 \times 10^{-5} \text{ cm}^2 \cdot \text{s}^{-1}$. The large water diffusion coefficient value suggests that water molecules diffuse very easily through our *ortho*-CPN channel.

***ortho*-CPN Interactions with Surrounding Lipid Bilayer.** The *ortho*-CPN interacts with the surrounding lipid bilayer through two kinds of contacts. At the middle region of the lipid bilayer, they interact with each other by hydrophobic contacts. At the two ends of the lipid bilayer, hydrogen bonding interactions were found. Analysis of the 10 ns MD trajectory revealed two types of long-lived hydrogen bonds, viz., those formed between the oxygen

atoms of the phosphate groups and the indole NH group of L-Trp or with the amide group of L-Gln; and those formed by the carbonyl group of the lipid with the L-Trp and L-Gln residues. The anchoring interactions of the lipid bilayer molecules with L-Gln and L-Trp residues may contribute to the tilt of the tube. The end subunit of the *ortho*-CPN is anchored via a hydrogen bond between the oxygen of phosphate or carbonyl group and the Trp or Gln. The number of hydrogen bonds between DMPC and R8 is bigger than that between DMPC and R1 (Figure 5). This could be the structural determinant for the observed slight distortion of subunits R7 and R8. These interactions result in the slight distortion in the subunits R7 and R8. Overall, the mode of hydrogen bonding interactions between the *ortho*-CPN subunits and the surrounding lipid bilayer molecules are similar to that reported for the gramicidin channel and octapeptide tube embedded in a lipid membrane.^{18,32}

The Transportation Mechanism of 5-FU across *ortho*-CPN. As depicted in Figure 6A, the pulling force was first averaged around zero at the beginning of SMD simulations. This force increased and formed different local peaks when 5-FU passed through each subunit of *ortho*-CPN. The force reached the maximum when 5-FU was passing through the subunit R7 and R8 near the outer end. Correspondingly, the distance between the center of mass (COM) of 5-FU and the geometry center of the tube featured an eight ladder decrease landscape when 5-FU passed through each subunit. Finally, 5-FU passed through the entire tube, and the pulling force decreased sharply to near zero. The “sawtoothed” pulling force profiles and “ladder” style walking of 5-FU (Figure 6A) revealed that 5-FU spanned each APR in a way of “hopping” through the whole tube. The pulling force increased when the aromatic plane of 5-FU became perpendicular to the hydrophobic APR as there was a molecular friction among 5-FU, water and the hydrophobic APR. The pulling force decreased when 5-FU went through the neighboring MPR as hydrogen bonds were formed among 5-FU, the inner wall of the nanotube and the diffusing water molecules. Such rise-and-fall of the pulling force appeared repeatedly as the 5-FU went through different APRs and MPRs, making the 5-FU hopping along the axis of the *ortho*-CPN.

Figure 6B shows several critical kinds of interactions between 5-FU and the *ortho*-CPN. The direct hydrogen bond

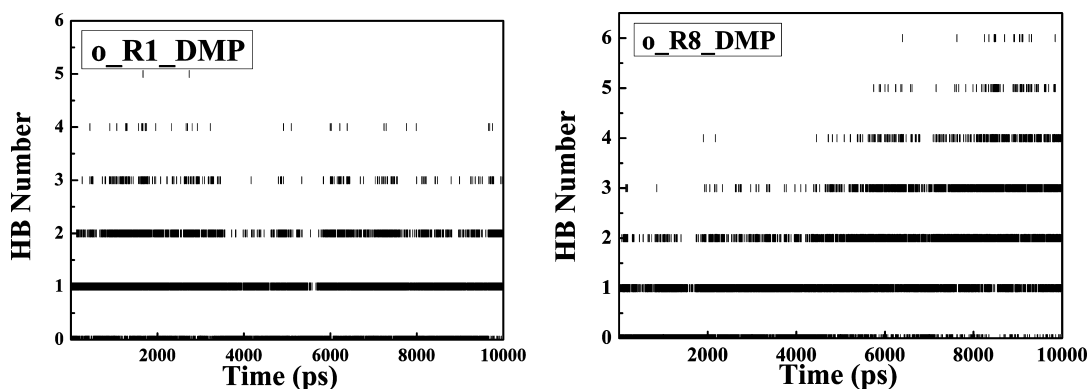


Figure 5. Time-evolutionary hydrogen bonding between *ortho*-CPN and the lipid bilayer.

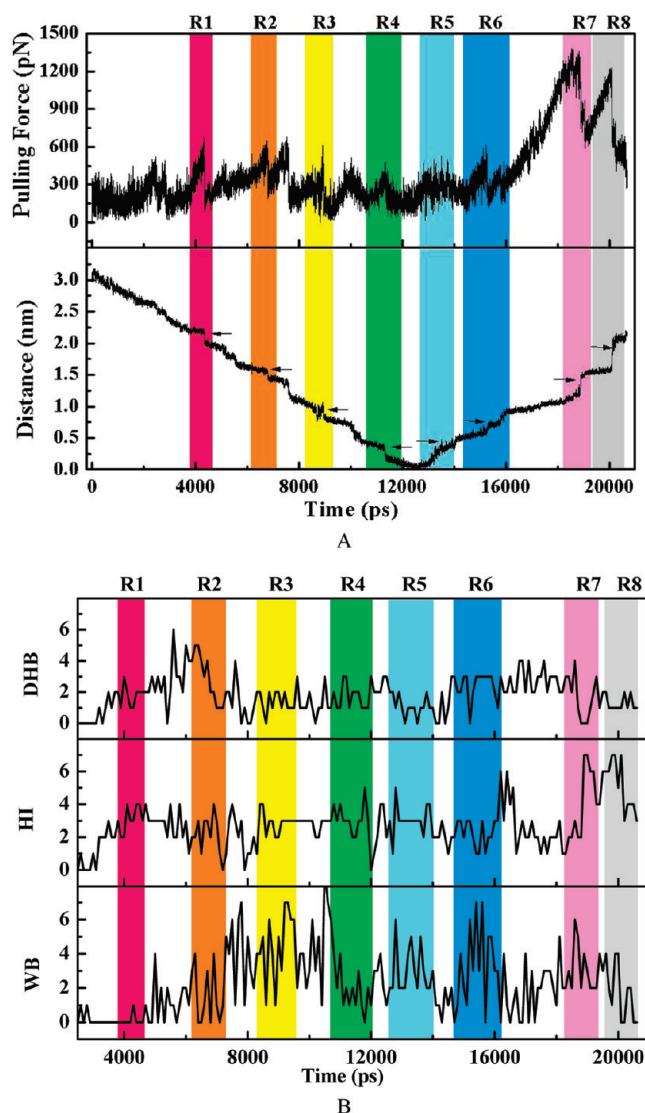


Figure 6. (A) The pulling force profile and distance feature between the center of mass of 5-FU and the geometry center of the nanotube. (B) The direct hydrogen bond (DHB), hydrophobic interactions (HI) and water bridges (WB) between 5-FU and *ortho*-CPN along the whole SMD simulations. Note: A hydrogen bond between 5-FU and CPN ($D-H\cdots A$) is defined if the intermolecular distances are $R_{D-A} \leq 3.3 \text{ \AA}$, $R_{H-A} \leq 2.6 \text{ \AA}$, and the donor-acceptor angle is $D-H\cdots A \geq 90^\circ$, and the $H\cdots A-AA$ angle is $\geq 90^\circ$, where AA is the atom attached to the acceptor; the van der Waals contact of nonpolar atoms ($R_{C-C} \leq 4.0 \text{ \AA}$) was used to define the hydrophobic interaction; the water bridge exists if several water molecules could form a hydrogen bond network with 5-FU and CPN.

(DHB), hydrophobic interactions (HI) and water bridges (WB) between 5-FU and *ortho*-CPN were tracked along the whole SMD simulations. When moving across each subunit of *ortho*-CPN, the interaction between 5-FU and *ortho*-CPN changed from one kind to another, including alternative old hydrogen bond breaking and new hydrogen bond formation. The number of DHB in MPR is generally bigger than that

in APR, showing an intrinsic driving force for the hopping of 5-FU. The number of DHB is about 2–3 on average when 5-FU walked from subunit 2 to subunit 6. The number of DHB increased to 3–4 when 5-FU went through the MPR between subunit 6 and subunit 7. The 5-FU dwelled 2 ns at this kink region of *ortho*-CPN before it went to the final steps across subunit 7 and subunit 8. The number of DHB dramatically increased to 6 when 5-FU was passing through the kink structure around subunits 7 and 8. Meanwhile, the number of WB strikingly changed from 2 to 6 when 5-FU dwelled in the region of subunits 7 and 8. There is no obvious difference between the kink region and rest of the tube. The above analyses fully illuminate the importance of the interaction between 5-FU, diffusing inner water and the inner wall of tube in the transport process of 5-FU.

Figure 7A represents typical snapshots from SMD trajectory for 5-FU hopping through the *ortho*-CPN, and Figure S4 in the Supporting Information shows the tracked changes of angle between the 5-FU plane and the axis of the nanotube. These results confirm the perpendicular jump of 5-FU in each APR as well as the reorientation of 5-FU in each MPR. Such a hopping mode of 5-FU was also confirmed by the potential energy profile for 5-FU moving through the *ortho*-CPN (Figure 7B). The characteristics of the hopping mode of 5-FU as shown in Figure 7 are consistent with the mode of changes for the pulling force and for the critical interactions among 5-FU, diffusing waters and the interior wall of the nanotube (Figure 6).

As displayed in Figure 6A, the maximum force pulling 5-FU through the tube ranged from 250 to 550 pN before 5-FU entered the region of the last two subunits (subunit 7 and subunit 8). The pulling force dramatically increased to 1250 pN and formed two peaks when 5-FU arrived at subunit 7 and subunit 8. As discussed above, the nanotube formed a minor kink at subunit 7 and subunit 8, but the artificial pulling force did not change its direction at the kink region. As a result, 5-FU was trapped in the kink and a bigger artificial force was needed to help the 5-FU molecule escape from the trap. Several questions could be raised as to how the 5-FU escaped from the kink structure of the nanotube. For example, how did the pulling force affect the 5-FU moving trajectory? Did the kink structure in the end subunit affect the translocation rate of 5-FU? Was the energy well located at the kink region? To answer these questions, the binding free energy profiles of 5-FU with *ortho*-CPN along with SMD simulations were calculated using the AutoDock4.0 scoring function. The calculated results are shown

- (31) Stout, D. G.; Steponkus, P. L.; Bustard, L. D.; Cotts, R. M. Water permeability of *Chlorella* cell membranes by nuclear magnetic resonance: Measured diffusion coefficients and relaxation times. *Plant Physiol.* **1978**, *62* (1), 146–151.
- (32) Woolf, T. B.; Roux, B. Molecular dynamics simulation of the Gramicidin channel in a phospholipid bilayer. *Proc. Natl. Acad. Sci. U.S.A.* **1994**, *91* (24), 11631–11635. Roux, B. Computational studies of the gramicidin channel. *Acc. Chem. Res.* **2002**, *35* (6), 366–375.

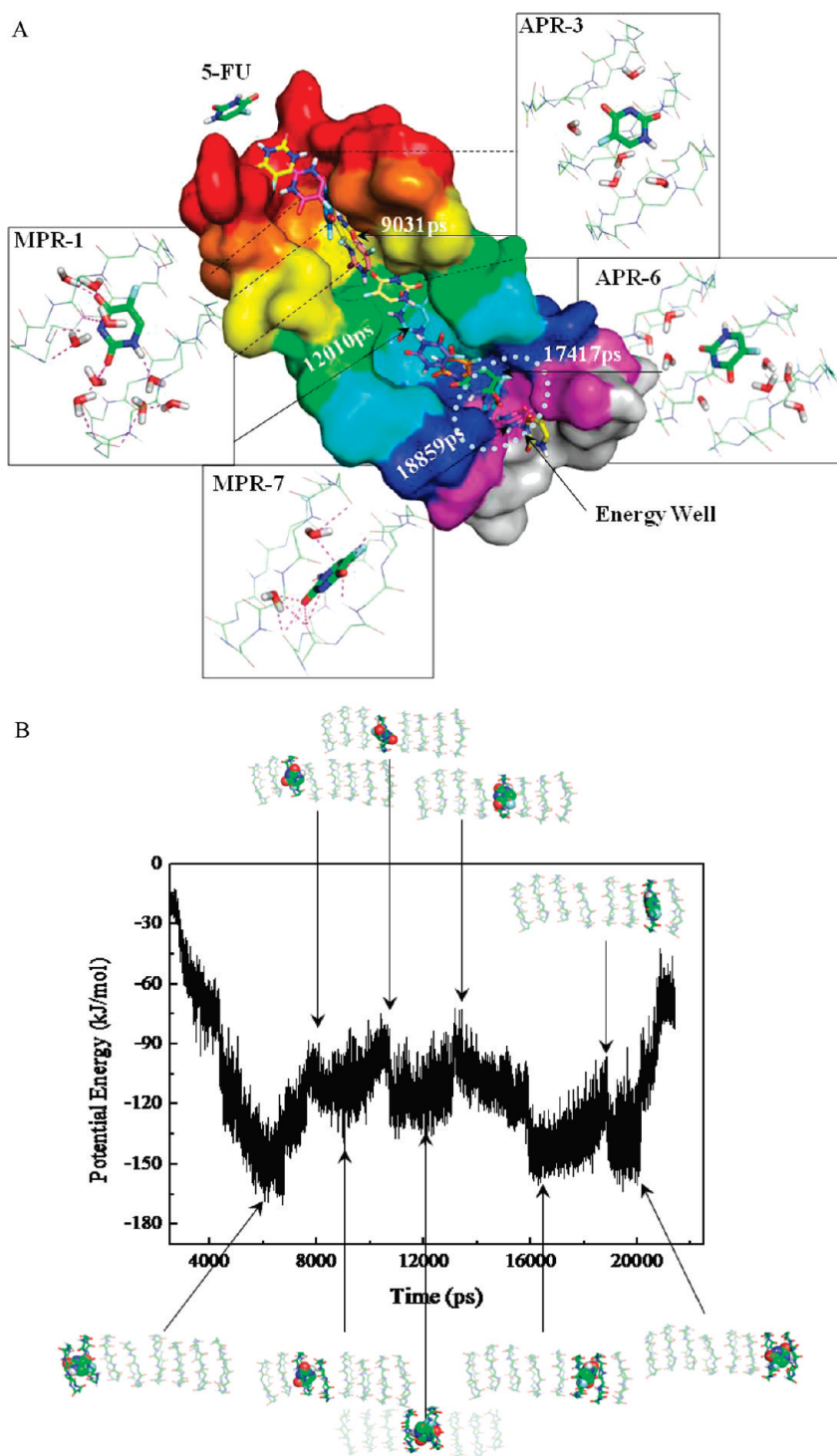


Figure 7. (A) The representative snapshots of 5-FU going through the nanotube along the whole SMD simulations. (B) The potential energy profile for 5-FU transported through the nanotube by SMD simulations.

in Figure 8. Corresponding to the peak of pulling force at the kink region, the calculated binding free energy based on the reaction coordinate became as low as -4.9 kcal/mol. Obviously, there must be an energy well at this kink region of the *ortho*-CPN (indicated in Figure 7A). The existence of such an energy well at the kink region certainly slowed down the transporting of 5-FU across the nanotube. Other studies also suggested that structural kinking significantly delays water diffusion in the gramicidin channel which has

apparently “single-file” inner water structure.³³ However, Ghadiri et al.¹⁶ indicated that the alternating 1–2 water structure (i.e., APR-1; MPR-2) inside the octapeptide channel may enhance the water diffusion. Based on our experimental observations and the results of SMD simulations as described

(33) Roux, B.; Prodhom, B.; Karplus, M. Ion transport in the gramicidin channel—molecular dynamics study of single and double occupancy. *Biophys. J.* **1995**, *68* (3), 876–892.

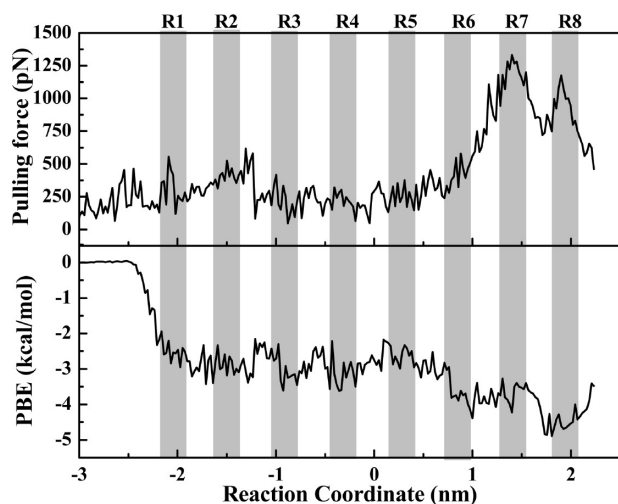


Figure 8. The pulling force and calculated binding free energy profile for 5-FU interacting with *ortho*-CPN.

above, the *ortho*-CPN is able to transport water molecules and small drug molecules, and the transporting process should be much faster than that of the gramicidin channel or octapeptide channel. The slower walking process of 5-FU at the kink region as well as the relatively large “wiggle” space of the tube (10 Å in the diameter) at this local region enabled more water molecules surrounding the polar 5-FU (Figure 4). Because of the dynamic nature of water molecules (Figure 4), the entropic effects may help the 5-FU molecule escape from the kink region and move further along the nanotube

Ghadiri et al.¹⁵ tested the glucose transport of the cyclo-octapeptide tube by glucose-entrapped unilamellar lipid vesicle studies, but the molecular mechanism of glucose transporting has not been well addressed. The reported transporting mechanism of Na⁺ and K⁺ along the octapeptide channel is quite different from the hopping process for 5-FU transported by *ortho*-CPN.^{6,8} The slower transporting of Na⁺ and K⁺ along the octapeptide channel was attributed to the electrostatic interactions of Na⁺ or K⁺ with the negatively charged carbonyl at the wall of the octapeptide nanotube. In addition, many more water molecules were found surrounding the Na⁺ and K⁺ along the octapeptide channel, while the 5-FU molecule formed a hydrogen bonding network with the interior wall of the MPR region of *ortho*-CPN in the present study.³⁴

Conclusion

In this work, we synthesized *cyclo*[(Trp-D-Leu)₄-Gln-D-Leu] peptide subunits. The studies on drug loaded liposomes showed that 5-FU could quickly be transported across the lipid bilayers after adding cyclic peptides into the aqueous suspensions of large unilamellar liposomes. The result combined with earlier investigations confirmed that the actual transport of 5-FU was facilitated by *ortho*-CPN in a lipid environment.

Computational studies have brought insights on the structural and dynamical characteristics of the synthetic CPN,

and molecular mechanism of 5-FU transportation by the nanotube by CMD simulations and SMD simulations. Detailed analyses of the whole CMD trajectory revealed that the β -sheetlike cylindrical tube conserved its hollow tubular structure by means of intersubunit hydrogen bond network between the carbonyl and amide groups on the backbone of the tube. The CMD simulation demonstrated that CPN tilted about 50° with respect to the normal of the bilayer. The value of this tilting angle is close to the reported tilt angle of 39° for octapeptide nanotube by ATR-IR spectroscopy measurements.

The robust hydrogen bond network formed by the carbonyl and amide group of the backbone in CPN, the inner diffusing water and the oxygen of the phosphate on surrounding lipid contributed to the stability and tilt of the tube. On average, 38 diffusing water molecules were found in the tube and most of them preferred to reside in the middle zone (MPR) of neighboring cyclic peptide subunits. Analysis of the motion of diffusing water molecules in the tube gives a diffusion constant of $1.068 \times 10^{-5} \text{ cm}^2 \cdot \text{s}^{-1}$. This value of diffusion coefficient is approximately half of the value of self-diffusion coefficient of bulk water ($2.3 \times 10^{-5} \text{ cm}^2 \cdot \text{s}^{-1}$), 2.4 times the value for octapeptide tube, and 42 times the value of water molecules diffusing inside the gramicidin A channel. Such a large value of diffusion coefficient indicates a bulk-like behavior of the inner diffusing water.

SMD simulation was conducted to uncover the transport process of 5-FU across the lipid bilayer. Based on our simulation results and analyses, we proposed a molecular mechanism for the transport of 5-FU across CPN. During the transporting process, 5-FU hopped over each APR and resided in each MPR by switching from hydrophobic interactions with the interior wall of the nanotube to hydrogen bonding interactions with carbonyl group and amide group of each MPR. The characteristics of the pulling force profile of SMD simulations and the potential energy profile of the *ortho*-CPN confirmed the hopping style of 5-FU transporting. Finally, 5-FU was transported to the outer end of the nanotube by escaping from the energy well located around the kink region at subunits 7 and 8 of *ortho*-CPN. Both our experimental and computational results demonstrated that *ortho*-CPN is an ideal transporter for the delivery of antitumor drug 5-FU to tumor cells.

Acknowledgment. The authors gratefully acknowledge Dr. M. R. Ghadiri for providing us the initial molecular model of the cyclic peptide nanotube and Dr. Weihua Li for his helpful discussions upon SMD simulation. This work is financially supported by the National Science Foundation of China (NSFC) (No. 30672546, 20702009) and partly by the National Key Basic Research Program of China (No. 2007CB935800, 2009CB930300).

Supporting Information Available: Figures S1–S4 as discussed in the text. This material is available free of charge via the Internet at <http://pubs.acs.org>.

MP100274F

(34) Asthagiri, D.; Bashford, D. Continuum and atomistic modeling of ion partitioning into a peptide nanotube. *Biophys. J.* **2002**, *82* (3), 1176–1189.